WILEY

Saturated areas through the lens: 2. Spatio-temporal variability of streamflow generation and its relationship with surface saturation

Marta Antonelli[1,2] | Barbara Glaser[2,3] | Adriaan J. Teuling[1] | Julian Klaus[2] | Laurent Pfister[2]

[1]Hydrology and Quantitative Water Management Group, Wageningen University & Research, Wageningen, The Netherlands

[2]Catchment and Eco-Hydrology Research Group, Luxembourg Institute of Science and Technology, Esch/Alzette, Luxembourg

[3]Department of Hydrology, University of Bayreuth, Bayreuth, Germany

Correspondence
Marta Antonelli, Hydrology and Quantitative Water Management Group, Wageningen University & Research, Wageningen 6700, The Netherlands.
Email: marta.antonelli88@gmail.com

Abstract

Investigating the spatio-temporal variability of streamflow generation is fundamental to interpret the hydrological and biochemical functioning of catchments. In humid temperate environments, streamflow generation is often linked to the occurrence of near stream surface saturated areas, which mediate hydrological connectivity between hillslopes and streams. In this second contribution of a series of two papers, we used salt dilution gauging to investigate the spatio-temporal variability of streamflow in different subcatchments and for different reaches in the Weierbach catchment (0.42 km^2) and explored the topographical controls on streamflow variability. Moreover, we mapped stream network expansion and contraction dynamics. Finally, we combined the information on the spatio-temporal variability of streamflow with the characterization of riparian surface saturation dynamics of seven different areas within the catchment (mapped with thermal infrared imagery, as presented in our first manuscript). We found heterogeneities in the streamflow contribution from different portions of the catchment. Although the size of the contributing area could explain differences in subcatchments' and reaches' net discharge, no clear topographic controls could be found when considering the area-normalized discharge. This suggests that some local conditions exert control on the variability of specific discharge (e.g., local bedrock characteristics and occurrence of perennial springs). Stream network dynamics were found not to be very responsive to changes in catchment's discharge (i.e., total active stream length vs. stream outlet discharge relationship could be described through a power law function with exponent = 0.0195). On the contrary, surface saturation dynamics were found to be in agreement with the level of streamflow contribution from the correspondent reach in some of the investigated riparian areas. This study represents an example of how the combination of different techniques can be used to characterize the internal heterogeneity of the catchment and thus improve our understanding of how hydrological connectivity is established and streamflow is generated.

1 | INTRODUCTION

The spatio-temporal variability of surface saturated areas and its impact on the hydrological behaviour of catchments have been on top of research agendas for several decades. Surface saturated areas are recognized as key areas in generating run-off in humid temperate regions (Ambroise, 2004; Hewlett, 1961)—mediating the onset and offset of hydrological connectivity between hillslopes and streams (Birkel, Tetzlaff, Dunn, & Soulsby, 2010; Bracken & Croke, 2007; Tetzlaff et al., 2007). In these environments, the development of surface saturated areas is primarily due to the occurrence of saturation excess (Dunne & Black, 1970a) in near stream areas with low relief and shallow water table (i.e., riparian zone) and up to the previously dry low-order channels (Bracken & Croke, 2007; Dunne, Moore, & Taylor, 1975; Montgomery & Dietrich, 1989). Both riparian surface saturated areas and stream networks are known to be highly dynamic (Dunne et al., 1975; Godsey & Kirchner, 2014; Shaw, 2016; Whiting & Godsey, 2016), quickly extending in response to precipitation and fostering the establishment of hydrological connectivity between the riparian zone and the stream—eventually triggering run-off generation (Bracken & Croke, 2007). Moreover, riparian surface saturated areas and stream network expansion and contraction dynamics reflect local groundwater (GW) dynamics. The spatial extent of riparian surface saturated areas can be considered as a valuable indicator of the hydrological state of the catchment and, in particular, of GW storage during baseflow conditions (Ambroise, 2016; Gburek & Sharpley, 1998; Myrabø, 1997). Similarly, stream network dynamics have been defined as a visible expression of subsurface processes otherwise hidden (Godsey & Kirchner, 2014). For these reasons, an accurate characterization of surface saturation and stream network dynamics is required to fully interpret the hydrological behaviour of catchments in humid temperate environments and to accurately predict run-off dynamics and associated flowpaths.

Understanding how run-off is generated within a catchment and which features, namely, catchment topography, geology, vegetation, and climate, control its variability is crucial to interpret catchment responses and stream water biogeochemical signatures and fluxes (Bergstrom, Jencso, & McGlynn, 2016; Pinay, 2005). Some experimental studies on this subject have adopted catchment discretization into defined landscape units such as hillslopes, riparian areas, and streams (Jencso et al., 2009; McGlynn, 2003; McGlynn & McDonnell, 2003; McGlynn, McDonnell, Seibert, & Kendall, 2004), providing fundamental information on run-off source area dynamics in terms of hillslope–riparian–stream (HRS) connectivity (defined as water table continuity across hillslope, riparian zone, and stream). These studies helped to clarify the relative role of different landscape units as spatial sources of run-off and the importance of riparian zones in regulating the portion of "new" and "old" water in stormflow (McGlynn et al., 2004; McGlynn & McDonnell, 2003). Other studies have focused on characterizing spatial and temporal variability of run-off by measuring discharge along continuous stream reaches (Anderson & Burt, 1978; Bergstrom, Jencso, et al., 2016; Floriancic et al., 2018; Genereux, Hemond, & Mulholland, 1993; Huff, O'Neill, Emanuel, Elwood, & Newbold, 1982; Kuraś, Weiler, & Alila, 2008; Payn, Gooseff, McGlynn, Bencala, & Wondzell, 2012; Shaw, Bonville, & Chandler, 2017). Unlike the studies employing catchment discretization, these studies take into account the dynamics of surface water (cf. Blume & van Meerveld, 2015), specifically the increase or decrease of streamflow between two measurement points. When applied over a whole stream network, this approach has the advantage of providing a general indication of heterogeneities in streamflow generation within the catchment. This heterogeneity can be directly linked to hydrologic dynamics, structure, and vegetation to understand how different processes are integrated along the stream to produce the total discharge volume at the outlet.

In humid temperate regions, spatio-temporal variability of streamflow is very often linked to the location and temporal variability of surface saturated areas (Bracken & Croke, 2007). However, studies combining variability in streamflow generation with surface saturation dynamics are extremely rare (Shaw et al., 2017; Ward, Schmadel, & Wondzell, 2018). Moreover, these studies tend to focus only on stream network dynamics. To the best of our knowledge, riparian surface saturation dynamics have only been investigated in relation to measurements of discharge at the catchment outlet or in relation to GW level fluctuations (Birkel et al., 2010; Dunne & Black, 1970b; Lana-Renault, Regüés, Serrano, & Latron, 2014; Latron & Gallart, 2007; Martínez Fernández, Ceballos Barbancho, Hernández Santana, Casado Ledesma, & Morán Tejeda, 2015; Tanaka, Yasuhara, Sakai, & Marui, 1988). The study of Kirnbauer and Haas (1998) in an Alpine catchment is a unique exception in this respect. They used stream gauges downstream of surface saturated areas to quantify their contribution to run-off. Combining a detailed description of surface saturation dynamics with the investigation of streamflow variability along the stream network could provide new insights on the spatial and temporal variability of HRS connectivity in humid temperate environments and, in particular, on the role of valley bottoms in regulating this connectivity. Additional experimental investigation along this line of work is needed across catchments with a range of geological and climate conditions to advance our understanding of surface saturation dynamics and its link to run-off generation.

The main obstacle to comparing surface saturation dynamics with streamflow dynamics along the stream network stems from the need to map surface saturation at the same temporal resolution to which streamflow is measured and for different locations within a restricted timeframe. Even though time consuming, mapping the active portion of the stream network can be achieved by walking along the stream and recording the active/inactive portions using a GPS receiver (Godsey & Kirchner, 2014; Shaw, 2016). More challenging is the mapping of riparian surface saturation, where classic approaches such as field surveys based on the "squishy boot" method may not provide an adequate spatio-temporal resolution (Pfister, McDonnell, Hissler, & Hoffmann, 2010). In this regard, recent technological development is represented by ground-based remote sensing techniques (i.e., thermal infrared [TIR] or digital imagery) with which surface saturation can be mapped at a higher temporal (i.e., minutes to weeks) and spatial (i.e., centimetres to metres) resolution (Glaser et al., 2016; Glaser, Antonelli, Chini, Pfister, & Klaus, 2018; Pfister et al., 2010; Silasari, Parajka, Ressl, Strauss, & Blöschl, 2017).

Here, we investigate the link between surface saturation dynamics (read as both riparian surface saturation and dynamics of expansion and contraction of the active portion of the stream network) and streamflow generation in the Weierbach catchment in Luxembourg. The Weierbach catchment is a long-term studied catchment, nowadays considered as a reference catchment for rainfall-dominated mountainous catchments (Zuecco, Penna, & Borga, 2018). The catchment's hydrological response is influenced by a storage threshold (Martínez-Carreras et al., 2016), and it is characterized by a single spiky peak in case of dry antecedent conditions and by a first spiky peak followed by a broader peak of longer duration in case of wet antecedent conditions (Martínez-Carreras et al., 2016; Wrede et al., 2014). The riparian zone in this catchment presents seasonally dynamic surface saturated areas whose possible influence on the connectivity and hydrological response of the system has never been clarified.

This contribution is the second in a series of two papers. Here, we leverage (a) information obtained by monitoring the spatio-temporal dynamics of riparian surface saturation via TIR imagery (as presented in our first manuscript; Antonelli, Glaser, Teuling, Klaus, & Pfister in review) and (b) manual mapping of the dynamic stream network and incremental flow gauging at different flow stages (this manuscript). We employ these datasets to

1. investigate the spatial distribution of streamflow generation in the Weierbach catchment during different flow conditions and compare the streamflow contributions from different subcatchments and individual reaches between consecutive streamflow gauging points;
2. explore the relationship between surface saturation and streamflow contributions from different reaches; and
3. understand how streamflow contributions from different stream reaches are controlled by riparian and upslope topographic characteristics (i.e., terrain indices extracted from a digital elevation model [DEM]).

Our findings will be discussed in light of the current perceptual model of the Weierbach catchment (Martínez-Carreras et al., 2016; Scaini et al., 2018; Wrede et al., 2014) and compared with previous research in a broader context.
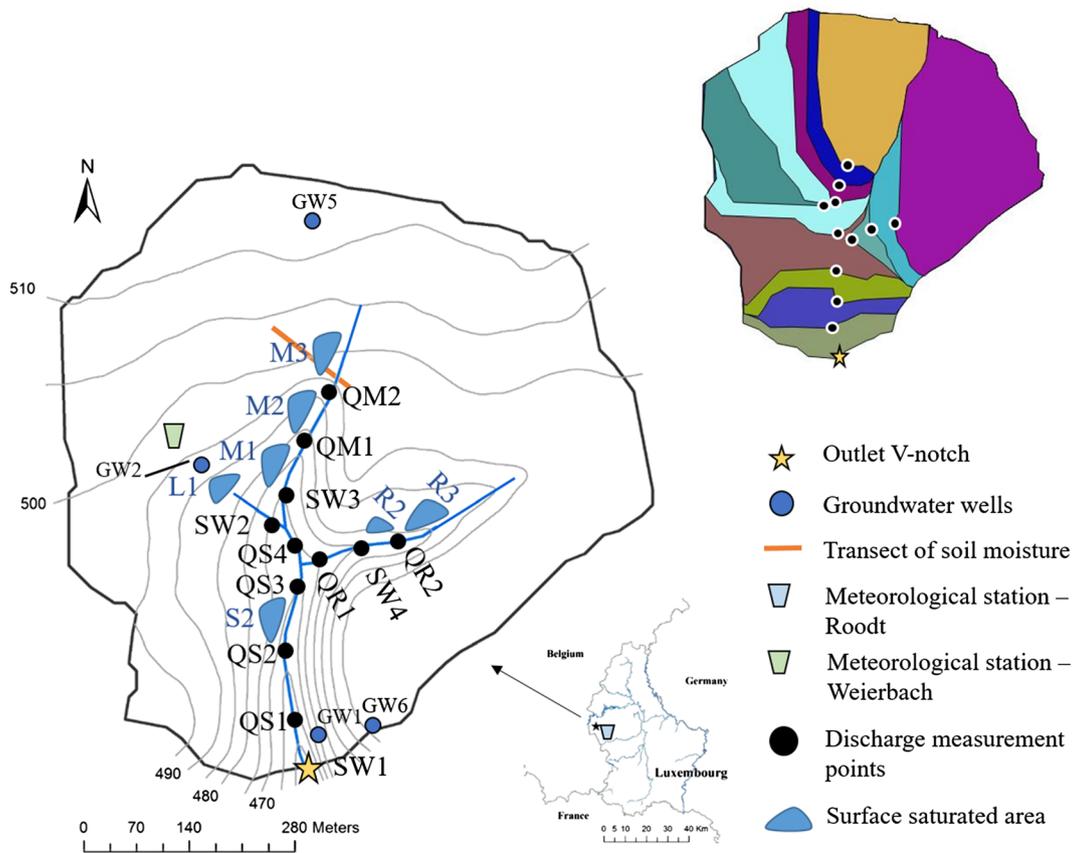
2 | STUDY SITE—WEIERBACH CATCHMENT

The Weierbach catchment (0.42 km^2) is an experimental catchment located in the North-West of the Grand Duchy of Luxembourg (49°49′N, 5°47′E, see Figure 1). The catchment is fully forested, with vegetation dominated by oak and beech trees and spruce mainly on the eastern side of the catchment. The climate is semioceanic, with an annual average precipitation of 918 mm (2011–2017). Detailed information about the soil and bedrock characteristics and seasonal hydrological response is reported in the companion paper by Antonelli et al. in review, as well as in several other studies (Gourdol, Clément, Juilleret, Pfister, & Hissler, 2018; Martínez-Carreras et al., 2016; Wrede et al., 2014). Here, we briefly summarize the information from the first manuscript about the riparian zone and the seven distinct areas within the catchment where we monitored riparian surface saturation (Figure 1). The riparian zone has been identified by taking into account shifts in dominant vegetation, occurrence of shallow clay-loam, organic soil (i.e., Leptosol), and a gentle slope (<5°). The riparian zone covers roughly 1.2% of the total catchment area (0.42 km^2). The seven riparian areas have been divided into three groups: areas L1, M3, and R3 as "stream Source Areas with Perennial springs (PSA)," areas M2 and S2 as "Areas along the stream with Perennial Springs (PSpA)," and areas M1 and R2 as "Areas along the stream with Non-Perennial Springs (N-PSpA)." These groups have been defined based on some intrinsic characteristics of the areas, such as location within the catchment, riparian width, and presence of perennial springs (see section 4.2 and table 1 in Antonelli et al. in review).

3 | MATERIALS AND METHODS

3.1 | Hydro-meteorological measurements and catchment storage calculation

Hydro-meteorological measurements of stream discharge at the outlet, GW levels, and soil volumetric water content (VWC) are carried out in the Weierbach catchment since 2002. The reader is referred to Antonelli et al. in review, for a complete description of the used instrumentation and data recording frequency, as well as for details on the hydro-meteorological measurements and estimations (i.e., reference evapotranspiration and catchment storage) employed in this study. Time series describing the hydrological response of the catchment for the study period from November 2015 to December 2017 are reported in the results section 4.1 in Antonelli et al. in review.

FIGURE 1 Map of location and instrumentation of the Weierbach catchment and location of the points along the stream where dilution gauging discharge measurements have been carried out. Upper right panel: contributing area to the different dilution gauging discharge measurement points

3.2 │ Monitoring of saturated areas in the riparian zone and stream network dynamics

Riparian surface saturation and stream network dynamics have been surveyed simultaneously, weekly, or fortnightly from November 2015 to December 2017. Riparian surface saturation has been monitored in seven different locations via ground-based TIR imagery, and its dynamic has been characterized through postprocessing of the TIR camera outputs (i.e., sequential images or videos) following the methodology outlined in Glaser et al. (2018). The riparian surface saturated areas were seasonally variable and were found to be particularly responsive to GW fluctuations. The development of surface saturation in the seven different areas is influenced by local riparian morphology that leads to small differences in the relationship between surface saturation and outlet discharge observed for the different areas. For a thorough characterization of the dynamics of riparian surface saturation, the reader is referred to the accompanying manuscript (cf. results section 4.4 in Antonelli et al. in review).

We mapped stream network dynamics manually by walking along the stream channel (within a few hours) and tagging the locations where stream flow initiated or ceased (Figure 2). We considered as locations of starting stream flow only those where water was flowing downstream, excluding locations where the water was just ponding without flowing. Tag positions along the stream were translated into

coordinates on a high-resolution LIDAR DEM (~5 cm) by manually measuring the distance between the tags and between the tags and ground control points that could be identified both in the field and in the DEM (i.e., trees and logs). Tag positions were recorded manually because of very poor GPS reception in the forested study site. For each tagged location, we calculated its distance from the outlet and

FIGURE 2 Illustration of tagging used to indicate initiation of stream flow in one of the headwater reaches. Tags were added during field visits under different wetness conditions. White arrows are added to indicate flow direction (photo: Marta Antonelli)

elevation. For each date of survey, we calculated the total active stream length (as per Whiting & Godsey, 2016).
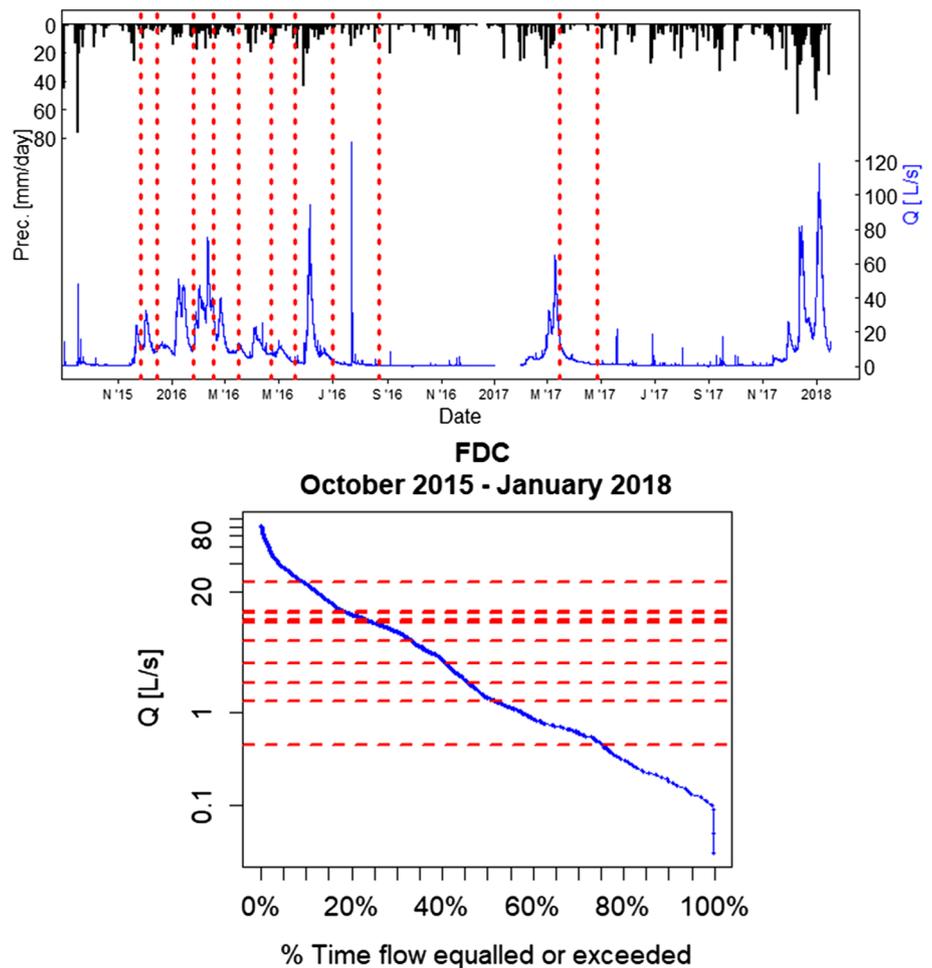
3.3 | Salt dilution gauging

Stream discharge was measured via salt dilution gauging at 12 locations along the stream network (Figure 1). The measurements were carried out within a few hours on 11 dates with no rain and contrasting hydrological states (Figure 3). Salt dilution gauging (Day, 1976) is a common method for measuring discharge in small streams with irregular streambed morphology (Moore, 2004). Measurement locations were selected based on two criteria: (a) include a surface saturated area between the upstream and downstream measurement locations and (b) maximize the possibility for complete mixing of the injected salt solution and stream water between the injection point and the measurement location (i.e., by injecting just upstream of a riffle or a narrowing of the stream section), which is an important requisite for salt dilution gauging (Day, 1977; Moore, 2004). We injected a solution of a known amount of NaCl. Electrical conductivity was recorded at the discharge measurement locations using a WTW Multi 3420 device, equipped with a TetraCon 925 probe (Xylem Analytics, Weilheim, Germany).

Replicates of the salt dilution gauging were carried out for 15 of the measurements, covering different flow states and measurement locations. In these cases, a second injection was carried out after the stream electrical conductivity returned to its background value. We found an average error between the two replicates of ~3%, with a minimum of 0% and a maximum of 10%, which was sufficient for our application.

3.4 | Data analysis

The discharge values (L/s) retrieved via salt dilution gauging at the different locations along the stream were used to characterize the spatial and temporal variability of streamflow generation in the catchment. We compared the streamflow at the outlets of the different subcatchments (i.e., catchment area above each discharge measurement location—Figure 1 upper right panel) in terms of area-normalized discharge (specific discharge—mm/day). We calculated the net discharge between two measurement locations (i.e., for a reach—Figure 1 upper right panel) as their difference in discharge (L/s). In order to compare reaches of different lengths, we expressed the net discharge as specific discharge (mm/day) and normalized it by the reach stream length (m). Similarities between specific discharge produced by each subcatchment and similarities between normalized specific discharge contributions from the different reaches were tested with the Mann–Whitney–Wilcoxon test ($\alpha = 0.05$). The test was applied by taking into account the subcatchments against each other for the dates where a

FIGURE 3 Streamflow dynamics at the catchment outlet and days of salt dilution gauging (dashed red lines). The same days are reported along the flow duration curve (FDC; 2-year study period) for the catchment outlet

measure of discharge (or net discharge) was available for the considered pair. The same procedure was followed for the reaches. Spearman's rank correlation test rho (ρ; α = 0.01) was applied in order to test monotonic relationships between the subcatchments' specific discharge and the other hydrometric measurements (i.e., stream discharge at the outlet, estimated catchment storage, GW levels, and soil VWC—daily-averaged values) and between the normalized specific discharge contribution of the different reaches and the hydrometric measurements (i.e., daily-averaged values).

We used multiple linear regression analyses to investigate which topographic characteristics influenced discharge (L/s) and specific discharge (mm/day) contributions of the different subcatchments and reaches (non-normalized values). We extracted several topographic features from a DEM (5-m resolution) and from a high-resolution LIDAR DEM (~5-cm resolution). We extracted topographic features for the different subcatchments and for the portion of the catchment draining between the two measurement locations defining a reach (i.e., upslope catchment area). Specifically, we considered catchment area, riparian area, percentage of riparian area, riparian buffer (riparian area/hillslope area), median slope (only for the reaches because too homogeneous between the subcatchments), percentage of steep slope (i.e., >15°), median elevation, median flow length (only for the subcatchments), and reach length (only for the reaches). The models were ran for each discharge measurement date and averaged through

time. Variance inflation factor analysis and backward selection were carried out to select the significant variables to retain in the models.

To investigate the relationship between stream network dynamics and stream outlet discharge, we related outlet discharge and stream length dynamics of the three headwater areas and tested the occurrence of monotonic relationships with Spearman's rank correlation (α = 0.01). We also related outlet discharge and the total active stream length (i.e., total stream length considering the entire catchment) and fitted a power law equation (stream length = $a * Q^{\beta}$) to this relationship following the approach of Godsey and Kirchner (2014). The total active stream length versus discharge relationship can provide an estimation of how much the total active stream length changes (in percentage) with changes in discharge. This estimation is represented by the β power law scaling exponent. Following a similar approach, we related the total active stream length and estimated catchment storage and GW level (measured in well GW5 on the plateau—the closest well to two out of three monitored headwater areas). We fitted equations that approximated the trend of these relationships. The goodness of fit of all the fittings was tested with Kolmogorov–Smirnov test (p value > 0.1). All the hydrometric variables are daily averages.

Finally, we explored the relationship between riparian surface saturation dynamics in the seven investigated areas and (a) normalized specific discharge contributions and (b) net discharge (expressed as percentage of the outlet discharge) of the correspondent reach. Note
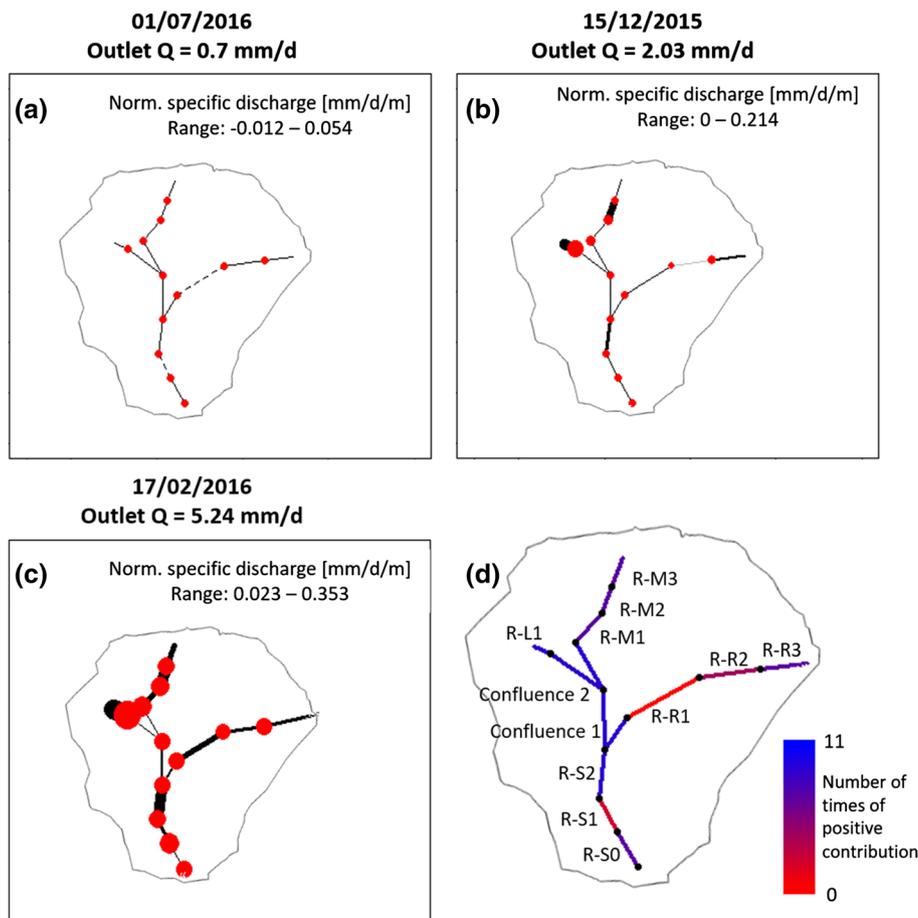
FIGURE 4 Distribution of specific discharge contributions across the Weierbach catchment. (a) July 1, 2016, (b) December 15, 2015, and (c) February 17, 2016. Line width is proportional to the magnitude of reaches' specific discharge normalized to unit reach length, considering the range of contributions for each measurement date (in mm/day/m; reported in the graphs). The variable length of the headwater segments reflects the stream dynamics in these sections. Dashed lines represent sections with losing conditions, and grey lines represent absence of contributions. Diameters of red points are proportional to subcatchment specific discharge. (d) The map provides an indication of the number of time the reaches contributed positively to streamflow considering all stream gauging dates (11). The map also reports the names for reaches. For the discharge measurement point names, we refer to Figure 1

that the number of observations that could be used to explore these relationships was consistently lower than for the other investigated relationships. This was due to the low quality of the TIR images collected during some of the stream gauging dates. Therefore, and due to its low statistical significance, we avoided any quantification of the strength of this relationship. However, we believe that a description of the trends that could be observed from the scatterplots (cf. Figures 8 and 9) would provide us with valuable information.

4 | RESULTS

4.1 | Spatio-temporal variability of streamflow

Streamflow within the catchment was found to be highly variable in both space and time. The normalized specific discharge contributions of the different reaches and subcatchments' specific discharge are shown for 3 days of stream gauging (Figure 4). The selected dates can be considered as representative of the system during dry (Figure 4a), intermediate (Figure 4b), and wet (Figure 4c) conditions. In general, the relative difference between normalized specific discharge contributions from the different reaches was smaller during drier conditions compared with wetter conditions. For example, the percentage relative difference between the reach with the smallest contribution and the one with the largest contribution was 5.5% on 07/01/2016 (Figure 4a) and 14.3% on 02/17/2016 (Figure 4c). During dry conditions, some reaches exhibited a negative contribution (i.e., R-S1 and R-R1 in Figure 4a). The same reaches shifted to a positive contribution during intermediate wetness conditions, and R-L1 and R-M2 started to contribute considerably more than others (Figure 4b). During wet conditions, the contribution of these reaches increased further, and R-M1 and R-M3, R-R1, R-R2, and R-R3, and R-S2 and R-S1 became more active as well (Figure 4c).

Considering all the measurement dates, some reaches were found to contribute positively to streamflow more frequently than others (i.e., R-L1 and R-S2 in Figure 4d). Similarly, some reaches showed overall higher variability in contribution (i.e., R-S2, R-L1, R-M2, and R-R1) compared with others (Figure 5a). Between the reaches with most variable contribution, R-L1 and R-M2 were found to be particularly similar (Mann–Whitney–Wilcoxon test p value = .7). Specific discharge contributions of the different subcatchments appeared to be quite homogeneous within the same stream gauging dates (Figure 4). Only the subcatchment with outlet in point SW2 produced systematically higher specific discharge than the other subcatchments, even though this difference was not statistically significant (Mann–Whitney–Wilcoxon test p value always higher than.05; Figure 5b). Overall, subcatchments' contribution was generally less variable in space and in time than observed for the different reaches.

The values of specific discharge of the different subcatchments showed generally a higher positive monotonic relationship with the other hydrometric measurements than the normalized specific discharge contributions of the different reaches as seen from the correlations described hereafter. In particular, all subcatchments' discharge were well correlated between each other (Spearman's rank test ρ not
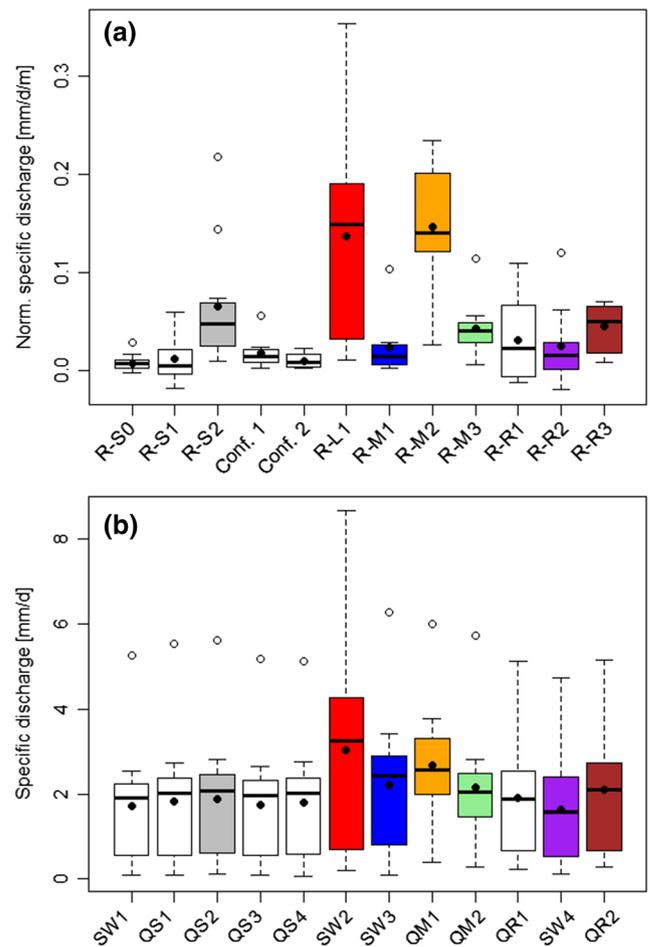
FIGURE 5 Distribution of specific discharge contributions. (a) Distribution of normalized specific discharge contributions across the different reaches. (b) Distribution of specific discharge of the different subcatchments. The colours of the boxplots in both panels refer to the colours assigned to the different riparian surface saturated areas in Antonelli et al. (). For the reaches, a colour is assigned if the reach includes the correspondent riparian surface saturated area; for the subcatchments, a colour is assigned if the subcatchment outlet is right downstream the correspondent riparian surface saturated area

lower than 0.83), and, with exception of the subcatchment with outlet in point QR2, they were all well correlated with discharge at the catchment outlet and estimated catchment storage (ρ not lower than 0.8). GW levels measured in Locations 2 and 3 were correlated with all the subcatchments' discharge (ρ not lower than 0.82 except for QR2 subcatchment), whereas GW levels in Locations 5 and 6 were mainly correlated with the subcatchments with outlet to the central stream (i.e., from SW1 to SW3) and in SW4 ($0.74 \leq \rho \leq 0.93$). Soil VWC was less correlated with subcatchments' specific discharge in general, with VWC measured in the spruce-covered hillslope showing the better correlation with most of the subcatchments ($0.8 \leq \rho \leq 0.88$) and VWC measured in riparian location being correlated with none (nonsignificant correlations). When considering monotonic relationships between normalized specific discharge contributions of the

different reaches, we observed that reaches R-S0, R-S1, R-L1, R-M1, R-R2, and R-R3 were not correlated to other reaches and, except R-L1 and R-R3, never correlated with catchment outlet discharge, estimated catchment storage, or GW levels ($\rho \le 0.75$ or nonsignificant correlations). VWC never correlated with normalized specific discharge contributions of any reach, except for R-S2 (ρ not lower than 0.81). Also in this case, VWC measured in riparian location did not correlate with any reach (nonsignificant correlations).

4.2 | Stream network dynamics and relationship between riparian surface saturation and reaches' streamflow contribution

During the study period, the stream network never dried out completely. We observed only occasionally lack of flow at the outlet (e.g., in January 2017, when the stream was partially frozen) or moments in which appreciably downstream sections of the stream became ephemeral (e.g., in September 2016, the stream stopped flowing in proximity of the discharge measurement point "QS3" and started flowing again close to the surface saturated area S2). In general, we could always detect flow starting points at the three headwater locations, even though sometimes the water reinfiltrated after few metres.

Stream network expansion and contraction dynamics in the three headwater stream reaches (R-L1, R-M3, and R-R3) were all positively monotonically related to catchment's outlet discharge (Spearman's rank test ρ not lower than 0.81—Figure 6). R-L1 was the reach that expanded the least, with a difference between its

maximum and minimum observed starting points of about 8 m. In contrast, R-R3 extended about up to 60 m above its minimum observed starting point. R-M3 extended upward along both the main reach direction (i.e., "R-M3 centre" in Figure 6) and on the right (i.e., "R-M3 right" in Figure 6). In both cases, the reach extended about 30 m above its minimum observed starting point. We could observe one or more particularly stable flow starting points for all three headwater reaches (Figure 6). In R-L1, this point was located at about 383 m upward from the outlet. In R-M3, stable points were found at about 480 m upward from the outlet (common part of the reach), 503 m (central direction), and 502 m (right direction). In R-R3, stable points were at about 409 m and 425 m upward from the outlet.

The relationship between the total active stream length and outlet discharge could be adequately described with a power law equation—linear in a log–log space (Figure 7a, $\beta = 0.0195$; goodness of fit was tested with Kolmogorov–Smirnov test—p value > .1). This shows that the total active stream length did not respond linearly to unit changes of outlet discharge. For the relationship between the total active stream length and both estimated catchment storage and GW level, a linear equation better fitted the data (Figure 7b,c, R^2 = .94 and.9, respectively).
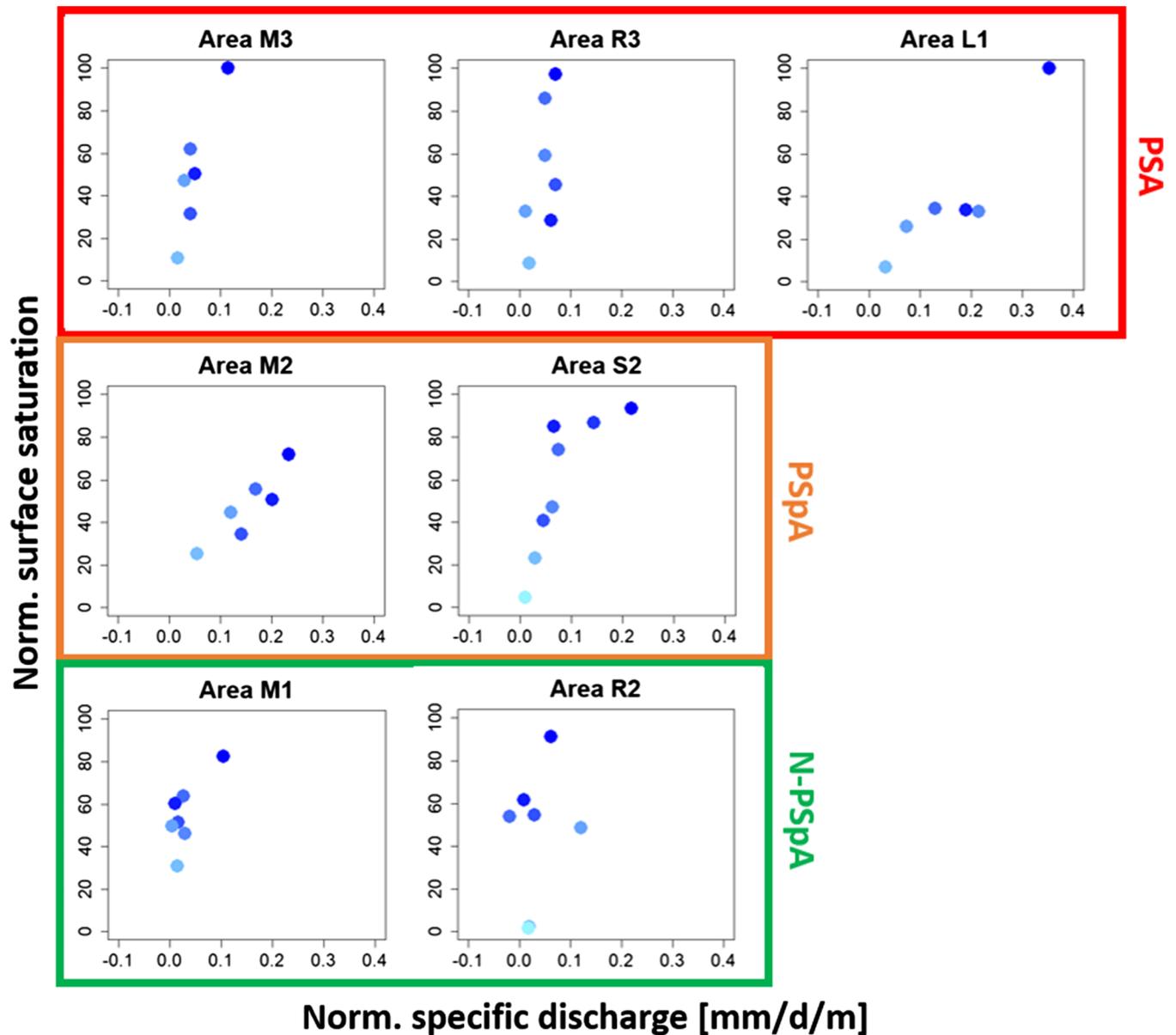
The relationships between surface saturation in the seven investigated riparian areas and streamflow contributions of the corresponding reaches showed some heterogeneities, especially when considering the normalized specific discharge contributions. For the areas L1, M2, and S2, we found a clear positive trend between extent of riparian surface saturation and normalized specific discharge
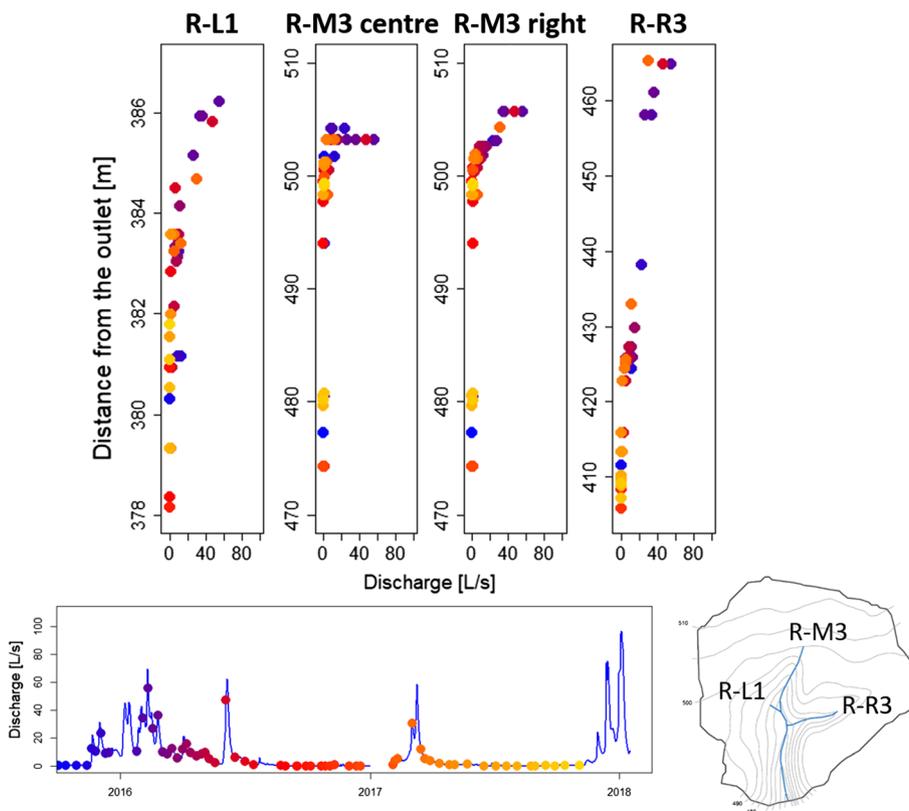
FIGURE 6 Dynamics of stream length expansion and contraction of the three headwater reaches in relation to catchment discharge at the outlet. The bottom panel shows the outlet discharge at the moments the flow starting locations have been mapped
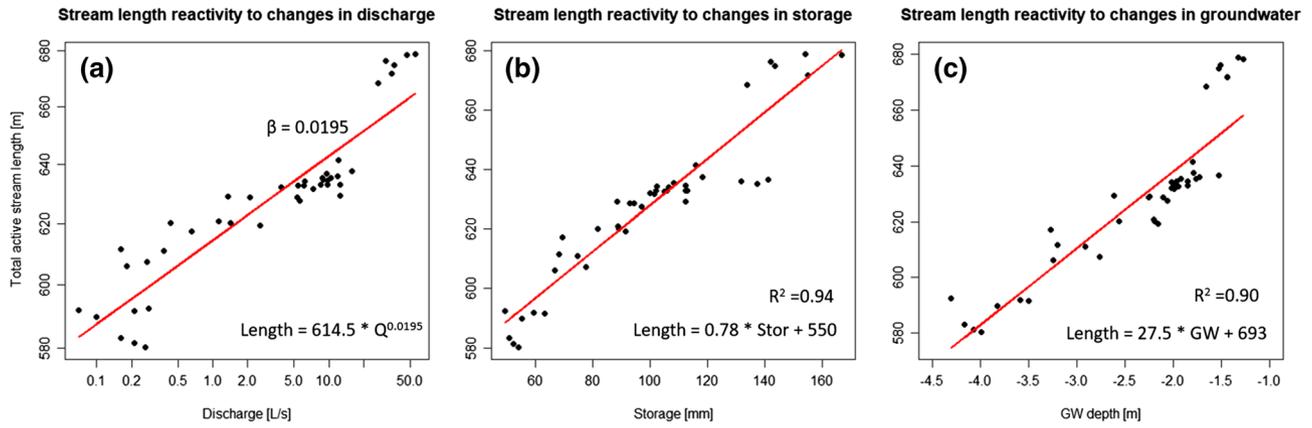
FIGURE 7 Relationships between stream length and catchment conditions. Shown are relations between total active stream length and discharge at the (a) outlet (in log–log space), (b) estimated catchment storage, and (c) groundwater (GW) depth

FIGURE 8 Relationship between normalized extent of surface saturation in the seven investigated riparian areas and normalized specific discharge contribution (mm/day/m) of the correspondent reach. Points' blue shades indicate observations during dryer (lighter blue shades) or wetter conditions (darker blue shades)
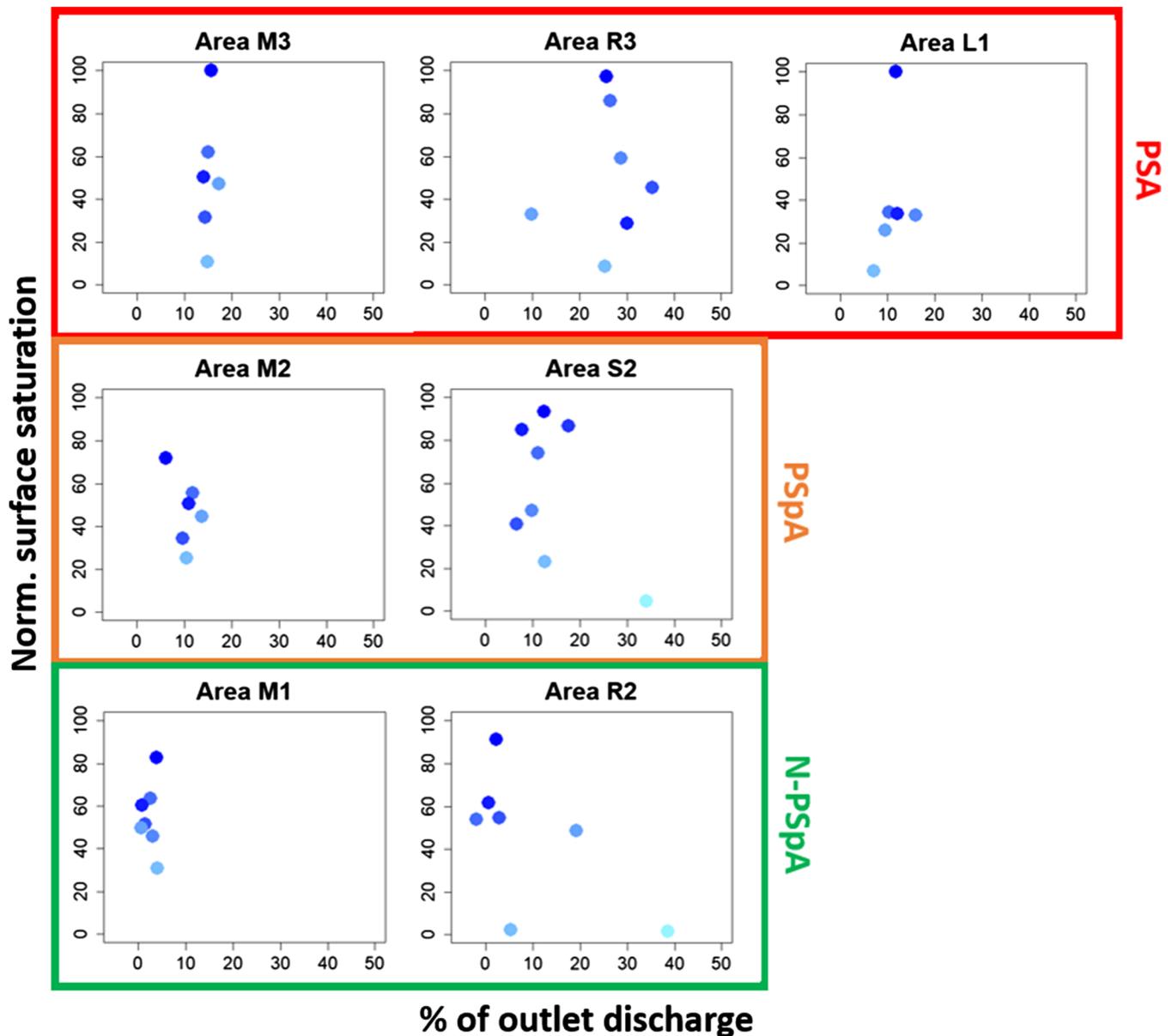
FIGURE 9 Relationship between normalized extent of surface saturation in the seven investigated riparian areas and net discharge (expressed as % of outlet discharge) of the correspondent reach. Points' blue shades indicate observations during dryer (lighter blue shades) or wetter conditions (darker blue shades)

contributions (Figure 8). Areas M3, R3, and M1 showed a slight positive trend, but normalized specific discharge contribution varied less compared with L1, M2, and S2, with the observations almost plotting on a vertical line. No particular trend was observed for area R2. When considering the relationship between extent of riparian surface saturation and net discharge of the reaches (percentage of outlet discharge), we found that areas M3, M2, M1, and L1 contributed to a quite constant percentage of the total catchment discharge, regardless of the dynamic riparian surface saturation (Figure 9). Areas R3, R2, and S2 showed more variability in their percentage contributions to total discharge with changes in riparian surface saturation. For all the areas, no clear trends are apparent from the relationships considering percentage of outlet discharge.

4.3 | Relationships between topography and streamflow contribution

A set of topographic characteristics have been initially considered in the multiple linear regression analyses for discharge and specific discharge of subcatchments (Table 1) and reaches (Table 2). After having accounted for collinearity between the variables, only catchment area, riparian buffer, median elevation, and percentage of steep slope were retained for the multiple linear regression analyses considering the subcatchments. For the multiple linear regression analyses relative to the reaches, only percentage of riparian area was excluded. Similarly, employing backward selection, different combinations of topographic variables were retained as significant variable for the model when considering different discharge measurement dates.

TABLE 1 Subcatchment topographic characteristics

Subcatchment	Area (m^2)	Riparian area (m^2)	% Riparian area	Riparian buffer	% Steep slope (>15°)	Median flowpath length (m)	Median elevation (m)
SW1	423,438	5,041	1.19	0.012	9.72	557	497
QS1	386,880	4,520	1.17	0.012	7.69	487	497
QS2	368,549	4,155	1.13	0.011	5.91	422	497
QS3	351,816	3,623	1.03	0.010	5.19	391	498
QS4	178,668	1,317	0.74	0.007	3.87	310	502
SW2	34,757	153	0.44	0.005	0.00	122	500
SW3	94,371	679	0.72	0.008	5.03	233	504
QM1	77,164	491	0.63	0.006	3.84	197	504
QM2	63,668	262	0.41	0.004	1.7	159	505
QR1	134,182	1,135	0.85	0.009	4.5	349	497
SW4	129,339	480	0.37	0.004	3.9	268	497
QR2	113,840	302	0.26	0.003	2.72	254	498

TABLE 2 Upslope catchment topographic characteristics for the portion of the catchment between the lowest and highest discharge measurement locations for every reach (i.e., upslope catchment)

Reach	Area (m^2)	Riparian area (m^2)	% Riparian area	Riparian buffer	Median slope (°)	% Steep slope (>15°)	Median elevation (m)	Reach length (m)
R-S0	16,869	522	3.09	0.02	14.3	19.58	483	56
R-S1	21,451	364	1.70	0.02	11.3	24.07	486	57
R-S2	16,733	532	3.18	0.033	6.4	10.34	490	75
Confluence 1	38,966	1,170	3.00	0.03	6.1	3.50	489	100
Confluence 2	49,540	153	0.44	0.01	4.5	0.12	500	87
R-L1	34,757	153	0.44	0.005	4.5	0.00	500	18.36 (avg)
R-M1	17,207	188	1.09	0.011	5.7	1.52	501	48
R-M2	13,496	229	1.69	0.02	5.7	2.62	498	43
R-M3	63,668	262	0.41	0.004	4.5	1.70	505	46.85 (avg)
R-R1	4,843	656	13.54	0.16	12.6	8.01	485	91
R-R2	15,499	178	1.15	0.012	5.7	4.22	493	53
R-R3	113,840	302	0.26	0.003	4.5	2.72	498	41.69 (avg)

Note. Reach length for the three headwater reaches is reported as an average.

Subcatchment area and reaches' upslope catchment area significantly predicted discharge (L/s; positive regression coefficient) in all the models (except for the 04/22/2016 reaches' model; Table 3—first two columns). Median subcatchment elevation was also identified as a good predictor of subcatchments' discharge (positive regression coefficient, except for the 11/26/2015 model), especially during dry and intermediate catchment wetness conditions. All models considering discharge as response variable were significant (p value ≤ .05) and explained a good proportion of the discharge variance (i.e., 98–99% for subcatchments' models and 44–94% for reaches' models).

The predictive power and significance of the models considering specific discharge (mm/day) as response variable were considerably lower (Table 3—third column). For the subcatchments, only seven out of the 11 models were significant (p value ≤ .05) and explained

between 35% and 78% of specific discharge variance. In these cases, median subcatchment elevation significantly predicted subcatchments' specific discharge most of the time (positive regression coefficient). All the models considering reaches' specific discharge were found to be not significant.

5 | DISCUSSION

Until now, previous research carried out in the Weierbach catchment has led to considerable advancement in our level of understanding of how its hydrological response is generated. Through modelling and tracer-based studies (Fenicia et al., 2014; Glaser et al., 2016; Klaus, Wetzel, Martínez-Carreras, Ector, & Pfister, 2015; Martínez Fernández

TABLE 3 Multiple linear regression analyses output

Date	Subcatchment Q (L/s)	Reaches Q (L/s)	Subcatchment Specific Q (mm/day)
11/26/2015	Area: 2.2×10^{-5}*** Elev: -8.6×10^{-2}*	Area: 2.8×10^{-5}*** Length: -1.9×10^{-2}*	Area: -3.0×10^{-6}**
12/15/2015	Area: 2.2×10^{-5}***	Area: 1.7×10^{-5}** Length: -2.3×10^{-2}** Area rip: 1.3×10^{-3}*	Nonsignificant
01/25/2016	Area: 2.5×10^{-5}***	Area: 2.0×10^{-5}**	Elev: 0.1*
02/17/2016	Area: 5.8×10^{-5}***	Area: 5.7×10^{-5}**	Nonsignificant
03/17/2016	Area: 3.0×10^{-5}***	Area: 2.7×10^{-5}**	Elev: 0.1*
04/22/2016	Area: 1.4×10^{-5}*** Elev: 1.0×10^{-1}*	Median slope: -0.7*	Elev: 8.4×10^{-2}*
05/19/2016	Area: 5.5×10^{-6}*** Elev: 3.9×10^{-2}*	Few data	Elev: 0.03** Steep slope: 0.02*
07/01/2016	Area: 8.6×10^{-6}***	Area: 5.8×10^{-6}**	Elev: 0.03**
08/23/2016	Few data	Few data	Few data
03/16/2017	Area: 3.0×10^{-5}***	Area: 2.9×10^{-5}**	Nonsignificant
04/27/2017	Area: 3.4×10^{-6}*** Elev: 1.6×10^{-2}*	Area: 3.0×10^{-6}***	Elev: 0.01** Steep slope: 0.01*

Note. Significant linear regression parameters are reported for the models run for the different dates taking into account subcatchments' and reaches' discharge (L/s; first two columns) and subcatchments' specific discharge (mm/day; third column). For each significant parameter, the regression coefficient and the statistical significance are shown.

*** p value < .001.
** p value < .01.
* p value < .05.

et al., 2015; Martínez-Carreras et al., 2016; Schwab, Klaus, Pfister, & Weiler, 2018; Wrede et al., 2014), it has been possible to develop a solid perceptual model of the catchment, being able to explain its dual hydrological behaviour and related water sources. With the exception of the parallel modelling study by Glaser, Antonelli, Hopp, and Klaus (2019) on surface saturated areas, all the observations made until now have been based on the hydrological response of the catchment observed at its outlet. This response integrates and perhaps smoothens possible intracatchment heterogeneity, providing only a lumped view of the catchment functioning. To date, we still lack information on the possible heterogeneity of small-scale processes taking place in the Weierbach catchment such as surface saturation dynamics occurring at the riparian–stream interface. Krause et al. (2017) highlighted the importance of characterizing catchments' eco-hydrological interfaces (e.g., the riparian zone) structuring mechanisms and processes in order to predict the occurrence and understand the importance of hydrological hotspots (or "control points") on larger scale processes. Here, we focused our attention on streamflow generation by separating the catchment into multiple—potentially—streamflow contributing portions. We aimed to better understand the spatial and temporal variability of streamflow within the catchment and how this information relates to the local dynamics of surface saturation.

Catchment area showed to be the dominant topographic control on subcatchments' and reaches' discharge. The same relationship has been reported in several studies (e.g., Anderson & Burt, 1978;

Bergstrom, McGlynn, Mallard, & Covino, 2016; Jencso et al., 2009; Payn et al., 2012). During dry and intermediate catchment wetness conditions, catchment median elevation was an additional significant positive predictor for subcatchments' discharge. This positive correlation is probably the result of the presence of losing sections of the stream within subcatchments with overall lower median elevation (e.g., in reach SW1–QS2 and QR1–SW4—cf. Figure 4a). We observed quite homogeneous specific discharge contributions from the different subcatchments (cf. Figure 4). Subcatchments' specific discharge was well correlated with the hydrometric measurements of outlet discharge, GW levels, and thus, estimated catchment storage. Consistent with observations by Seibert, Bishop, Rodhe, and McDonnell (2003), we found that the correlation between subcatchments' specific discharge and GW levels decreased with increasing distance of the wells from the stream (i.e., GW2 and GW3 generally better correlated with specific discharge than GW5 and GW6). In our case, this trend existed in particular for the most upstream subcatchments, which were the catchments exhibiting the highest variability in specific discharge contributions—probably because their dynamics were not mitigated by catchments' area overlap (as noted by Kuraś et al., 2008; cf. Figure 5b).

When considering subcatchments' and reaches' contributions as specific discharge, the significance of both topographic predictors and multiple linear regression models decreased dramatically, to the point that no significant models could be identified for the reaches. The only parameter that had a consistent significant positive predictive

power on subcatchments' specific discharge was median elevation, once again mainly during dry conditions. These results suggest the presence of one/several important controlling factor/factors on specific discharge—especially when considering the different reaches—which has/have not been taken into account. As the high spatial and temporal variability observed in the reaches' normalized specific discharge (cf. Figures 4 and 5a) and their variable relationship with the different hydrometric measurements suggest, the specific discharge produced by each reach could be the result of very location-specific factors. For example, the presence of perennial springs in some of the reaches often resulted in generally higher normalized specific discharge (cf. Figure 5a). These reaches were the ones corresponding to PSA and PSpA locations observed via TIR imagery (described in our first contribution). An exception was the reach "QR1-SW4," which was identified as a losing reach during low flow and appeared to be quite active in terms of normalized specific discharge during higher flow. This is probably due to the activation of temporary springs in the streambed during wetter conditions. The activation of a temporary spring additionally to the perennial ones could be observed via TIR imagery in area S2, which also became very active during wetter conditions (cf. Figure 4c). Spring location and the delivery of water from the hillslopes to the streams are likely substantially controlled by bedrock characteristics as schists/slate weathering degree, fractures' size and orientation within the catchment (Gourdol et al., 2018; Scaini et al., 2018), and/or presence of faults (Shaw, 2016; Whiting & Godsey, 2016). The aforementioned bedrock characteristics have been shown to be variable within the Weierbach catchment (Gourdol et al., 2018), representing a substantial source of variability that can be hardly disentangled.

The stream network was observed to be dynamic, but it was not very responsive to changes in catchment outlet discharge. Stream network dynamics in the three headwater locations showed to be well monotonically related to catchment outlet discharge (Figure 6). However, the relationship between the total stream length and catchment outlet discharge suggested relatively small responsiveness of the stream network to changes in discharge (i.e., the low β value in the power law relationship). This is typical of catchments with stream heads "anchored" by perennial springs (cf. Figure 6), as reported by Whiting and Godsey (2016) and Shaw et al. (2017). In accordance with the observations by Withing and Godsey (2016), we detected a higher stability in reaches L1 and M3 compared with R3 (cf. Figure 6), which was the headwater location with the smaller accumulation area during higher flow (likely to be supported by longer, deeper, and slower flowpaths) and a flatter topography. Even though stream network dynamics were found to not to be very responsive to changes in the outlet discharge, they were found to be very well correlated to estimated catchment storage and GW depth. This suggest the total active stream length to reflect subsurface processes variability rather than surface water dynamics at the outlet.

Riparian areas have their surface saturation positively correlated to normalized specific discharge from the correspondent reach. Antonelli et al. in review, questioned if the small differences detected in the riparian surface saturation development and dynamics of the different riparian areas (PSA, PSpA, and N-PSpA) reflected their degree of hydrological connectivity with the hillslopes. As previously observed, reaches corresponding to PSA and PSpA provided generally higher streamflow contributions than N-PSpA. Analysing how reaches' contribution varied in relation to riparian surface saturation variations (cf. Figure 8), we noticed that an increase in the amount of surface saturation in the riparian area corresponded to a positive increase in normalized specific discharge, this being especially visible in PSA and PSpA. This could be related to the fact that both surface saturation and streamflow contributions from the hillslopes are influenced by GW fluctuations (Antonelli et al., in review; Glaser et al., 2019, 2016; Martínez-Carreras et al., 2016; Wrede et al., 2014). The observed surface saturation versus streamflow contribution relationships may mirror the level of connectivity of the different areas to the subsurface system as suggested in the perceptual model of Antonelli et al. in review. GW level fluctuations are likely to influence both the saturation in the riparian zone and the streambed in all the areas (Glaser et al., 2019). Eventually, water exchange between the riparian zone and the stream may contribute to the maintenance of a positive relationship between surface saturation and streamflow contribution. An example is represented by the activation of temporal springs in the riparian zone and the connectivity of the exfiltrated GW to the stream. This could be observed for area S2, where a clear increase in surface saturation and streamflow contribution is visible in moments of high flow (cf. Figure 8—area S2). This sharp increase is very likely to correspond to moments of activation of a temporal spring observed at the hillslope foot in this area. At a lesser extent, this was also observed in areas M1 and L1. The effect of longitudinal connectivity (i.e., water contributions from upstream) was also reflected in the surface saturation versus streamflow contribution relationship: In area R2, this resulted in higher mapped surface saturation regardless whether the reach was gaining, losing, or not contributing to streamflow (e.g., Figure 8—area R2). It is difficult to understand if the extensive and stable surface saturation developing in PSA and PSpA is related to their high streamflow contribution. Although this could be the case during rainfall events, in moments when the system is not affected by the occurrence of precipitations, the level of surface saturation in one area and the streamflow generated by the correspondent reach seem not to really influence each other but rather be influenced by common factors as GW dynamics and springs locations. Note that because surface saturation has been quantified as percentage of saturated pixels and not as area, we could not quantify if areas with an absolute larger surface saturation provided more streamflow contribution than others.

The described positive relationship between surface saturation and streamflow contribution disappears when we consider the percentage contribution of a specific reach to the total catchment outlet discharge. We noticed that some areas contributed for very stable percentage of total discharge regardless of the general catchment wetness conditions and the level of surface saturation in the area (cf. Figure 9). A more stable percentage of contribution seemed to be associated to the reaches located in the middle and west part of the stream (i.e., reaches M3, M2, M1, and L1), in contrast to the reaches located in the east (R2 and R2) and lower part (S2) of the stream. As

previously mentioned, the investigations of Gourdol et al. (2018) employing soil drilling and electrical resistivity tomography revealed some heterogeneities in the subsurface structure of the Weierbach catchment. In particular, they have shown that the northern and western part of the catchment is characterized by overall thinner solum (i.e., "true soil," where pedogenic processes are dominant; cf. Gourdol et al., 2018) and shallower hard bedrock compared with the eastern portion of the catchment. This may determine differences in the way different sides of the catchment deliver water to the stream. However, the mechanism behind the consistency of the relative contribution of some specific reaches to the total catchment outlet discharge remains of difficult interpretation.

The key role of near stream surface saturation in mediating hydrological connectivity between hillslopes and streams has been acknowledged across a range of landscapes and climate conditions, such as—just to mention a few—catchments in boreal and temperate environments (Birkel et al., 2010; Devito, Creed, & Fraser, 2005; Tetzlaff et al., 2007), Mediterranean (Lana-Renault et al., 2014; Latron & Gallart, 2007; Niedda & Pirastru, 2014), and alpine environments (Kirnbauer & Haas, 1998; von Freyberg, Radny, Gall, & Schirmer, 2014). Similarly to what we observed in the Weierbach catchment, GW dynamics and local topography—and in some cases, the presence of perennial GW springs—have been recognized as the main controls on surface saturation dynamics in the majority of the aforementioned studies. Thus, we believe our results to provide a good representation of the spatio-temporal dynamics of surface saturation and streamflow generation occurring in most headwater catchments.

Recent studies have reaffirmed the need for catchments' interfaces to be characterized for their own processes and fluxes in order to have a better perception of where and when connectivity may take place in a catchment (Blöschl et al., 2019; Wohl et al., 2019). Failure in assessing possible heterogeneities may lead to erroneous processes conceptualization and discrepancies between processes observed at smaller scales and responses that may occur at larger scales (Krause et al., 2017; Ward & Packman, 2019). In this study—together with its accompanying manuscript—we go beyond the sole characterization of the surface saturation versus outlet baseflow discharge relationship of a catchment (Ambroise, 2016; Latron & Gallart, 2007). Our results suggest that a deeper understanding of the role played by riparian surface saturation in mediating hydrological connectivity along the HRS continuum (and how it translates into the total discharge volume observed at the outlet) is possible—probably only—if considering the riparian zone (and the multitude of its hydrological processes) as a complex feature of the system, rather than as a single homogeneous entity (as suggested by Ledesma et al., 2018). Interfaces in hydrology have been traditionally considered as a boundary condition (Blöschl et al., 2019) where complexity is commonly reduced for the sake of simplicity in experimental and conceptual model designs (Krause et al., 2017). However, Blöschl et al. (2019) also recognize the need to start looking for more typical cases where this simplification can be applied or not. In our catchment, we observed that, although the seasonal dynamics of surface saturation in the different investigated areas seem to be synchronous (Antonelli et al. in review), this does not

necessarily translate into similar hydrological behaviour in terms of streamflow contribution for all areas. This kind of variability is at the base of the difference between variable active and variable contributing areas (or periods) described by Ambroise (2004) and has important implications for investigating and modelling catchments' responses. This is fundamental in studies that focus on biogeochemical transformations occurring in the riparian zone (Blume & van Meerveld, 2015; Laudon et al., 2016; Ledesma et al., 2018). Indeed, variable dynamics of surface saturation could provide indications on potentially different buffer capacities of distinct riparian sections, both in terms of water quantity and quality.

6 | CONCLUSION

In this contribution, we have explored the spatio-temporal variability of streamflow generation in the Weierbach catchment. We investigated possible links to the occurrence and dynamics of surface saturation and active stream length. We carried out our investigations at a finer scale compared with previous studies and showed that a considerable level of heterogeneity can be found within a small, homogeneous (e.g., vegetation coverage and pedological and geological characteristics) headwater catchment.

We found that the net discharge contribution variability between different subcatchments and between different reaches could be explained by the contributing area. However, this was not the case when considering the area-specific discharge contribution of different subcatchments and reaches. In this case, no clear topographic control was able to explain the variability in contribution, suggesting that very local factors may influence streamflow generation, such as bedrock characteristics or the presence of perennial springs. We related the surface saturation dynamics observed within the catchment to the streamflow dynamics. The stream network expansion and contraction dynamics reflected the general wetness state of the catchment (i.e., they were related to GW fluctuations and changes in the estimated catchment storage), but they were not very responsive to changes in outlet discharge (i.e., perennial springs would "anchor" the channel head in specific locations for most of the time). Finally, we showed that the surface saturation versus streamflow contribution relationship in different riparian areas could mirror the degree of connectivity of the areas to the subsurface system.

Besides providing new information on subcatchment scale processes in the Weierbach catchment, we have shown that a combination of a thorough investigation of surface saturated area dynamics within the catchment through TIR imagery with sequential measurements of stream discharge can be used to improve our perception and understanding of the internal heterogeneity of catchments. Our approach is in line with the "Roadmap for Eco-hydrological Interface Research" proposed by Krause et al. (2017), because we applied a combination of approaches from different disciplines to investigate the complexity of the riparian–stream interface and identify hotspots of hydrological connectivity/streamflow generation. This information

is also fundamental in studies that have their focus on nutrients and tracers transport and eco-hydrological processes in the riparian zone.

Future research should focus on analysing and linking the observed catchment's internal heterogeneities with reference to stream water isotopic and chemical signature or through simulation approaches.

ACKNOWLEDGMENTS

CONFLICT OF INTERESTS

The authors declare that they have no conflict of interest.

DATA AVAILABILITY STATEMENT

Data used in this study are property of the Luxembourg Institute of Science and Technology. They are available upon request from the authors.

ORCID

Marta Antonelli https://orcid.org/0000-0001-9560-1981
Laurent Pfister https://orcid.org/0000-0001-5494-5753

REFERENCES

Ambroise, B. (2004). Variable 'active' versus 'contributing' areas or periods: A necessary distinction. *Hydrological Processes*, *18*(6), 1149–1155. https://doi.org/10.1002/hyp.5536

Ambroise, B. (2016). Variable water-saturated areas and streamflow generation in the small Ringelbach catchment (Vosges Mountains, France): The master recession curve as an equilibrium curve for interactions between atmosphere, surface and ground waters. *Hydrological Processes*, *30*(20), 3560–3577. https://doi.org/10.1002/hyp.10947

Anderson, M. G., & Burt, T. P. (1978). The role of topography in controlling. *Earth Surface Processes*, *3*, 331–344.

Antonelli, M., Glaser, B., Teuling, A. J., Klaus, J., & Pfister, L. (in review). Saturated areas through the lens: 1. Spatio-temporal variability of surface saturation documented through Thermal Infrared imagery.

Bergstrom, A., Jencso, K., & McGlynn, B. (2016). Spatiotemporal processes that contribute to hydrologic exchange between hillslopes, valley bottoms, and streams. *Water Resources Research*, *52*(6), 4628–4645. https://doi.org/10.1002/2015WR017972

Bergstrom, A., McGlynn, B., Mallard, J., & Covino, T. (2016). Watershed structural influences on the distributions of stream network water and solute travel times under baseflow conditions. *Hydrological Processes*, *30*(15), 2671–2685. https://doi.org/10.1002/hyp.10792

Birkel, C., Tetzlaff, D., Dunn, S. M., & Soulsby, C. (2010). Towards a simple dynamic process conceptualization in rainfall-runoff models using multi-criteria calibration and tracers in temperate, upland catchments. *Hydrological Processes*, *24*(3), 260–275. https://doi.org/10.1002/hyp.7478

Blöschl, G., Bierkens, M. F. P., Chambel, A., Cudennec, C., Destouni, G., Fiori, A., … Zhang, Y. (2019). Twenty-three unsolved problems in hydrology (UPH)—A community perspective. *Hydrological Sciences Journal*, *64*(10), 1141–1158. https://doi.org/10.1080/02626667.2019.1620507

Blume, T., & van Meerveld, H. J. I. (2015). From hillslope to stream: Methods to investigate subsurface connectivity. *Wiley Interdisciplinary Reviews Water*, *2*(3), 177–198. https://doi.org/10.1002/wat2.1071

Bracken, L. J., & Croke, J. (2007). The concept of hydrological connectivity and its contribution to understanding runoff-dominated geomorphic systems. *Hydrological Processes*, *21*(13), 1749–1763. https://doi.org/10.1002/hyp.6313

Day, T. J. (1976). On the precision of salt dilution gauging. *Journal of Hydrology*, *31*(3–4), 293–306. https://doi.org/10.1016/0022-1694(76)90130-X

Day, T. J. (1977). Observed mixing lengths in mountain streams. *Journal of Hydrology*, *35*(1–2), 125–136. https://doi.org/10.1016/0022-1694(77)90081-6

Devito, K. J., Creed, I. F., & Fraser, C. J. D. (2005). Controls on runoff from a partially harvested aspen-forested headwater catchment, Boreal Plain, Canada. *Hydrological Processes*, *19*(1), 3–25. https://doi.org/10.1002/hyp.5776

Dunne, T., & Black, R. D. (1970a). An experimental investigation of runoff production in permeable soils. *Water Resources Research*, *6*(2), 478–490. https://doi.org/10.1029/WR006i002p00478

Dunne, T., & Black, R. D. (1970b). Partial area contributions to storm runoff in a small New England watershed. *Water Resources Research*, *6*(5), 1296–1311. Retrieved from http://soilandwater.bee.cornell.edu/Research/VSA/papers/DunneWRR70.pdf

Dunne, T., Moore, T. R., & Taylor, C. H. (1975). Recognition and prediction of runoff-producing zones in humid regions. *Hydrological Sciences Bulletin*, *20*(3), 305–327. https://doi.org/Cited By (since 1996) 102\rExport Date 4 April 2012

Fenicia, F., Kavetski, D., Savenije, H. H. G., Clark, M. P., Schoups, G., Pfister, L., & Freer, J. (2014). Catchment properties, function, and conceptual model representation: Is there a correspondence? *Hydrological Processes*, *28*(4), 2451–2467. https://doi.org/10.1002/hyp.9726

Floriancic, M. G., van Meerveld, I., Smoorenburg, M., Margreth, M., Naef, F., Kirchner, J. W., & Molnar, P. (2018). Spatio-temporal variability in contributions to low flows in the high Alpine Poschiavino catchment. *Hydrological Processes*, *32*(26), 3938–3953. https://doi.org/10.1002/hyp.13302

Gburek, W. J., & Sharpley, A. N. (1998). Hydrologic controls on phosphorus loss from upland agricultural watersheds. *Journal of Environmental Quality*, *27*(2), 267. https://doi.org/10.2134/jeq1998.00472425002700020005x

Genereux, D. P., Hemond, H. F., & Mulholland, P. J. (1993). Spatial and temporal variability in streamflow generation on the West Fork of Walker Branch Watershed. *Journal of Hydrology*, *142*(1–4), 137–166. https://doi.org/10.1016/0022-1694(93)90009-X

Glaser, B., Antonelli, M., Chini, M., Pfister, L., & Klaus, J. (2018). Technical note: Mapping surface-saturation dynamics with thermal infrared imagery. *Hydrology and Earth System Sciences*, *22*(11), 5987–6003. https://doi.org/10.5194/hess-22-5987-2018

Glaser, B., Antonelli, M., Hopp, L., & Klaus, J. (2019). Intra-catchment variability of surface saturation—Insights from long-term observations and

simulations. *Hydrology and Earth System Sciences Discussions*, 1–22. https://doi.org/10.5194/hess-2019-203

Glaser, B., Klaus, J., Frei, S., Frentress, J., Pfister, L., & Hopp, L. (2016). On the value of surface saturated area dynamics mapped with thermal infrared imagery for modeling the hillslope-riparian-stream continuum. *Water Resources Research*, 52(10), 8317–8342. https://doi.org/10.1002/2015WR018414

Godsey, S. E., & Kirchner, J. W. (2014). Dynamic, discontinuous stream networks: Hydrologically driven variations in active drainage density, flowing channels and stream order. *Hydrological Processes*, 28(23), 5791–5803. https://doi.org/10.1002/hyp.10310

Gourdol, L., Clément, R., Juilleret, J., Pfister, L., & Hissler, C. (2018). Large-scale ERT surveys for investigating shallow regolith properties and architecture. *Hydrology and Earth System Sciences Discussions*, (December), 1–39. https://doi.org/10.5194/hess-2018-519

Hewlett, J. D. (1961). Soil moisture as a source of baseflow from steep mountain watersheds. *Southeastern Forest Experiment Station Asheville, North Carolina*, (132).

Huff, D. D., O'Neill, R. V., Emanuel, W. R., Elwood, J. W., & Newbold, J. D. (1982). Flow variability and hillslope hydrology. *Earth Surface Processes and Landforms*, 7(1), 91–94. https://doi.org/10.1002/esp.3290070112

Jencso, K. G., McGlynn, B. L., Gooseff, M. N., Wondzell, S. M., Bencala, K. E., & Marshall, L. a. (2009). Hydrologic connectivity between landscapes and streams: Transferring reach- and plot-scale understanding to the catchment scale. *Water Resources Research*, 45(4), 1–16. https://doi.org/10.1029/2008WR007225

Kirnbauer, R., & Haas, P. (1998). Observations on runoff generation mechanism in small Alpine catchments. *Hydrology, Water Resources and Ecology in Headwaters*, 248(248), 275–283.

Klaus, J., Wetzel, C. E., Martínez-Carreras, N., Ector, L., & Pfister, L. (2015). A tracer to bridge the scales: On the value of diatoms for tracing fast flow path connectivity from headwaters to meso-scale catchments. *Hydrological Processes*, 29(25), 5275–5289. https://doi.org/10.1002/hyp.10628

Krause, S., Lewandowski, J., Grimm, N. B., Hannah, D. M., Pinay, G., McDonald, K., ... Turk, V. (2017). Ecohydrological interfaces as hot spots of ecosystem processes. *Water Resources Research*, 53(8), 6359–6376. https://doi.org/10.1002/2016WR019516

Kuraś, P. K., Weiler, M., & Alila, Y. (2008). The spatiotemporal variability of runoff generation and groundwater dynamics in a snow-dominated catchment. *Journal of Hydrology*, 352(1–2), 50–66. https://doi.org/10.1016/j.jhydrol.2007.12.021

Lana-Renault, N., Regüés, D., Serrano, P., & Latron, J. (2014). Spatial and temporal variability of groundwater dynamics in a sub-Mediterranean mountain catchment. *Hydrological Processes*, 28(8), 3288–3299. https://doi.org/10.1002/hyp.9892

Latron, J., & Gallart, F. (2007). Seasonal dynamics of runoff-contributing areas in a small mediterranean research catchment (Vallcebre, Eastern Pyrenees). *Journal of Hydrology*, 335(1–2), 194–206. https://doi.org/10.1016/j.jhydrol.2006.11.012

Laudon, H., Kuglerová, L., Sponseller, R. A., Futter, M., Nordin, A., Bishop, K., ... Ågren, A. M. (2016). The role of biogeochemical hotspots, landscape heterogeneity, and hydrological connectivity for minimizing forestry effects on water quality. *Ambio*, 45, 152–162. https://doi.org/10.1007/s13280-015-0751-8

Ledesma, J. L. J., Futter, M. N., Blackburn, M., Lidman, F., Grabs, T., Sponseller, R. A., ... Köhler, S. J. (2018). Towards an improved conceptualization of riparian zones in boreal forest headwaters. *Ecosystems*, 21(2), 297–315. https://doi.org/10.1007/s10021-017-0149-5

Martínez Fernández, J., Ceballos Barbancho, A., Hernández Santana, V., Casado Ledesma, S., & Morán Tejeda, C. (2015). Procesos hidrológicos en una cuenca forestal del Sistema Central: cuenca experimental de Rinconada. *Cuadernos de Investigación Geográfica*, 31(0), 7. https://doi.org/10.18172/cig.1171

Martínez-Carreras, N., Hissler, C., Gourdol, L., Klaus, J., Juilleret, J., Iffly, J. F., & Pfister, L. (2016). Storage controls on the generation of double peak hydrographs in a forested headwater catchment. *Journal of Hydrology*, 543, 255–269. https://doi.org/10.1016/j.jhydrol.2016.10.004

McGlynn, B. L. (2003). Distributed assessment of contributing area and riparian buffering along stream networks. *Water Resources Research*, 39(4), 1–7. https://doi.org/10.1029/2002WR001521

McGlynn, B. L., & McDonnell, J. J. (2003). Quantifying the relative contributions of riparian and hillslope zones to catchment runoff. *Water Resources Research*, 39(11), SWC2-1. https://doi.org/10.1029/2003WR002091

McGlynn, B. L., McDonnell, J. J., Seibert, J., & Kendall, C. (2004). Scale effects on headwater catchment runoff timing, flow sources, and groundwater-streamflow relations. *Water Resources Research*, 40(7), 1–14. https://doi.org/10.1029/2003WR002494

Montgomery, D. R., & Dietrich, W. E. (1989). Source areas, drainage density, and channel initiation. *Water Resources Research*, 25(8), 1907–1918.

Moore, R. D. (2004). Introduction to salt dilution gauging for streamflow measurement: Part 1. *Streamline Watershed Management Bulletin*, 7(4), 20–23. https://doi.org/10.1592/phco.23.9.1S.32890

Myrabø, S. (1997). Temporal and spatial scale of response area and groundwater variation in Till. *Hydrological Processes*, 11(14), 1861–1880. https://doi.org/10.1002/(sici)1099-1085(199711)11:14<1861::aid-hyp535>3.0.co;2-p

Niedda, M., & Pirastru, M. (2014). Field investigation and modelling of coupled stream discharge and shallow water-table dynamics in a small Mediterranean catchment (Sardinia). *Hydrological Processes*, 28(21), 5423–5435. https://doi.org/10.1002/hyp.10016

Payn, R. A., Gooseff, M. N., McGlynn, B. L., Bencala, K. E., & Wondzell, S. M. (2012). Exploring changes in the spatial distribution of stream baseflow generation during a seasonal recession. *Water Resources Research*, 48(4), 1–15. https://doi.org/10.1029/2011WR011552

Pfister, L., McDonnell, J. J., Hissler, C., & Hoffmann, L. (2010). Ground-based thermal imagery as a simple, practical tool for mapping saturated area connectivity and dynamics. *Hydrological Processes*, 24(May), 3123–3132. https://doi.org/10.1002/hyp.7840

Pinay, G. (2005). Linking hydrology and biogeochemistry. *Progress in Physical Geography*, 3, 297–316.

Scaini, A., Hissler, C., Fenicia, F., Juilleret, J., Iffly, J. F., Pfister, L., & Beven, K. (2018). Hillslope response to sprinkling and natural rainfall using velocity and celerity estimates in a slate-bedrock catchment. *Journal of Hydrology*, 558, 366–379. https://doi.org/10.1016/j.jhydrol.2017.12.011

Schwab, M. P., Klaus, J., Pfister, L., & Weiler, M. (2018). Diel fluctuations of viscosity-driven riparian inflow affect streamflow DOC concentration. *Biogeosciences*, 15(7), 2177–2188. https://doi.org/10.5194/bg-15-2177-2018

Seibert, J., Bishop, K., Rodhe, A., & McDonnell, J. J. (2003). Groundwater dynamics along a hillslope: A test of the steady state hypothesis. *Water Resources Research*, 39(1), 1–9. https://doi.org/10.1029/2002WR001404

Shaw, S. B. (2016). Investigating the linkage between streamflow recession rates and channel network contraction in a mesoscale catchment in New York state. *Hydrological Processes*, 30(3), 479–492. https://doi.org/10.1002/hyp.10626

Shaw, S. B., Bonville, D. B., & Chandler, D. G. (2017). Combining observations of channel network contraction and spatial discharge variation to inform spatial controls on baseflow in Birch Creek, Catskill Mountains, USA. *Journal of Hydrology: Regional Studies*, 12(March), 1–12. https://doi.org/10.1016/j.ejrh.2017.03.003

Silasari, R., Parajka, J., Ressl, C., Strauss, P., & Blöschl, G. (2017). Potential of time-lapse photography for identifying saturation area dynamics on

agricultural hillslopes. *Hydrological Processes*, 31(21), 3610–3627. https://doi.org/10.1002/hyp.11272

Tanaka, T., Yasuhara, M., Sakai, H., & Marui, A. (1988). The Hachioji Experimental Basin Study—Storm runoff processes and the mechanism of its generation. *Journal of Hydrology*, 102(1–4), 139–164. https://doi.org/10.1016/0022-1694(88)90095-9

Tetzlaff, D., Soulsby, C., Waldron, S., Malcolm, I. A., Bacon, P. J., Dunn, S. M., … Youngson, A. F. (2007). Conceptualization of runoff processes using a geographical information system and tracers in a nested meso-scale catchment. *Hydrological Processes*, 21(10), 1289–1307. https://doi.org/10.1002/hyp.6309

von Freyberg, J., Radny, D., Gall, H. E., & Schirmer, M. (2014). Implications of hydrologic connectivity between hillslopes and riparian zones on streamflow composition. *Journal of Contaminant Hydrology*, 169, 62–74. https://doi.org/10.1016/j.jconhyd.2014.07.005

Ward, A. S., & Packman, A. I. (2019). Advancing our predictive understanding of river corridor exchange. *Wiley Interdisciplinary Reviews Water*, 6(1), e1327. https://doi.org/10.1002/wat2.1327

Ward, A. S., Schmadel, N. M., & Wondzell, S. M. (2018). Simulation of dynamic expansion, contraction, and connectivity in a mountain stream network. *Advances in Water Resources*, 114, 64–82. https://doi.org/10.1016/j.advwatres.2018.01.018

Whiting, J. A., & Godsey, S. E. (2016). Discontinuous headwater stream networks with stable flowheads, Salmon River basin, Idaho. *Hydrological Processes*, 30(13), 2305–2316. https://doi.org/10.1002/hyp.10790

Wohl, E., Brierley, G., Cadol, D., Coulthard, T. J., Covino, T., Fryirs, K. A., … Sklar, L. S. (2019). Connectivity as an emergent property of geomorphic systems. *Earth Surface Processes and Landforms*, 44(1), 4–26. https://doi.org/10.1002/esp.4434

Wrede, S., Fenicia, F., Martínez-Carreras, N., Juilleret, J., Hissler, C., Krein, A., … Pfister, L. (2014). Towards more systematic perceptual model development: A case study using 3 Luxembourgish catchments. *Hydrological Processes*, 29(12), 2731–2750. https://doi.org/10.1002/hyp.10393

Zuecco, G., Penna, D., & Borga, M. (2018). Runoff generation in mountain catchments: Long-term hydrological monitoring in the Rio Vauz Catchment, Italy. *Cuadernos de Investigación Geográfica*, 44(2), 397. https://doi.org/10.18172/cig.3327